Stable Isotopic Variability of Daily Precipitation from Yungui Plateau of Southwest China: Insights from Moisture Source and Rainout Effect

huawu Wu
Nanjing Institute of Geography and Limnology Chinese Academy of Sciences
Congsheng Fu (hwwu@niglas.ac.cn)
Nanjing Institute of Geography and Limnology Chinese Academy of Sciences
Cicheng Zhang
Hunan Normal University
Zhongwang Wei
Sun Yat-Sen University
Xinping Zhang
Hunan Normal University

Research Article

Keywords: Stable water isotopes, Rainout processes, HYSPLIT backward trajectory, Moisture source, Southwest monsoon

Posted Date: June 22nd, 2021

DOI: https://doi.org/10.21203/rs.3.rs-602537/v1

Abstract

Long-term continuous monitoring of precipitation isotopes has great potential to advance our understanding of mechanisms that determine stable isotope variability in hydrological processes of monsoon regions. This study presents a 4-year daily data set of precipitation isotopes from Yungui Plateau of southwest China, influenced by southwest monsoon and East Asian monsoon. The local meteoric water line [LMWL, δ^2H=8.12 (±0.04) $\delta^{18}O$+11.2(±0.4)] was established at the Tengchong (TC) site, which was similar to the global meteoric water line (GMWL, δ^2H=8 $\delta^{18}O$+10) indicating little secondary sub-cloud evaporation in the falling rain. Precipitation $\delta^{18}O$ exhibited significant inverse relationships with precipitation amount (r = -0.42) and air temperature (r = -0.43) throughout the entire period, which indicated that precipitation isotopic variability largely depended on the local meteorological conditions. Precipitation $\delta^{18}O$ values are characterized by remarkably seasonal variability: In the summer monsoon period, moisture sources primarily originated from BoB source towards TC site experiencing local moisture recycling over land. The air masses were derived from the northern region of Africa and East Asia with the longest transporting distance and cyclonic activity over the source region in the Fall-winter period characterized with the depleted $\delta^{18}O$ values. Precipitation $\delta^{18}O$ at the TC site was estimated by a Rayleigh fractionation model considering rainout over BoB and land (Myanmar) during the vapor advection, and local recycling processes consistent with the observed precipitation $\delta^{18}O$ values. These findings enhance our understanding of hydrological cycle in the Southwest monsoon regions and will potentially facilitate the interpretation of numerous isotopic proxy records from this region.

Significance Statement

The variability of the summer monsoon, its onset, duration, and failure directly determine the strong rainfall and drought in a given region and have great impacts on regional societies and agriculture. To better understand this variability, this study presented a 4-year daily data set of precipitation isotopes on the Yungui Plateau of Southwest China to explore atmospheric processes and moisture source that drive isotopic variability in this region. Precipitation $\delta^{18}O$ exhibited remarkably seasonal variability with higher values in pre-monsoon period and lower values in the Fall-winter period. In the summer monsoon period, moisture sources primarily originated from the Bay of Bengal (BoB) toward the TC site, experiencing rainout processes and local moisture recycling over land using Rayleigh fractionation model. These findings shed a new light on the temporal variations of precipitation stable isotopes and facilitate our understanding of hydrological cycle in the monsoon regions.

1 Introduction

The climate of Yungui Plateau in Southwest China is controlled by the westerlies and summer monsoon systems of southwest monsoon from Bay of Bengal (BoB) and East Asian monsoon from the South China Sea (SCS), characterized by seasonally strong rainfall and drought. The variability of the summer monsoon, its onset, duration, and failure have great impacts on regional societies and agriculture (Lin et al. 2015; Xu et al. 2002; Zhang et al. 2012). To better understand it, many researchers make huge attempts to reconstruct past climate and hydrology of the region by linking stable isotopes ($\delta^{18}O$ and δ^2H) records of paleoarchives (e.g., stalagmites and lacustrine sediments) to hydrological and meteorological conditions (Cheng et al. 2016; Tan et al. 2018; Xiao et al. 2014).

Stable isotopes ($\delta^{18}O$ and δ^2H) in precipitation provides valuable information about moisture source and atmospheric circulation patterns that give rise to the rainfall on regional and global scales, and can be used to reconstruct past climate conditions. The so-called “temperature effect” (e.g., a positive correlation between $\delta^{18}O$ and

local air temperature) has been widely reported in the mid- to- high latitudes (Aggarwal et al. 2004; Dansgaard 1964). According to this effect, the isotopic signals from paleoarchives have been widely considered as a key index of paleotemperature (Gao et al. 2015; Yao et al. 1996). By contrast, in lower latitudes characterized by the empirical "amount effect" (e.g., an anti-correlation between monthly precipitation amount and precipitation $\delta^{18}O$), historical changes in precipitation amount and local atmospheric humidity can be reconstructed in these regions (Pausata et al. 2011; Yadava et al. 2004). However, several literatures have showed the insignificant or even non-existent amount effect at some low-latitude stations impacted by the Indian summer monsoon (Breitenbach et al. 2010; Sengupta; Sarkar 2006). Hence, this finding gives rise to several controversies regarding the amount effect for paleoclimatic reconstruction. Unlike the remarkable temperature effect in the high-latitude regions, potential factors controlling precipitation stable isotopes in the mid-low latitude monsoon regions are complex, it is deficient to unravel the potential mechanisms of precipitation stable isotopes to climatic and environmental forcing dependent solely on the statistical relationships with local meteorological parameters.

Using the observational isotope data, numerous studies examined a variety of hydrological processes determining the isotopic variability in precipitation such as rainout along transport paths, moisture sources, local microphysical processes within the cloud and precipitation type at both the daily and seasonal scales (Aggarwal et al. 2016; Wang et al. 2016). However, lack of precipitation isotope data has been restricted the systematic evaluation of these processes controlling isotopic variability of the southwestern monsoon regions available at monthly intervals from a few stations operating under the Global Network on Isotopes in Precipitation (GNIP) program. Recently, the Chinese Network of Isotopes in Precipitation (CHNIP) has begun to monitor precipitation isotopes at 40 sites across China at event-based resolution (Liu et al. 2014; Yao et al. 2013). Although these data sets are applied to determine spatial isotopic patterns and regional meteoric water line (Bowen et al. 2019; Zhang et al. 2010), the data present large gaps in the space and time. This coarse spatial and temporal resolution of the GNIP and CHNIP dataset masks the impact of individual storms on the isotopic composition of precipitation (Bedaso; Wu 2020; Li et al. 2015; Wu et al. 2015). Hence, the high frequency of event-based precipitation isotopes will provide the opportunity to delineate the climate-isotope relationship and how moisture sources affect the isotopic compositions in precipitation, especially in the southwestern monsoon regions.

Several studies, however, focused on either the influence of large-scale convective activity, cloud formation mechanisms and condensation processes along air mass trajectories in determining changes in precipitation stable isotopes across various monsoon regions (Cai et al. 2018; Lone et al. 2020; Wei et al. 2018). So far, the limited study has yet been investigated how the rainout effect over the ocean and land influence precipitation isotopes variability locally (Rahul et al. 2016a; Wolf et al. 2020), which still remains unclear. To that end, observations of sea surface temperature (SST), precipitation, and overhead moisture along air mass trajectory from source regions are used to explore the drivers for precipitation isotopes variability in southwest China.

The study site [Tengchong (25.01N, 98.30E, 1648 m a.s.l.)] is located in the Yungui Plateau of Southwest China. Previous studies were conducted to identify the local meteorological derivers determining the precipitation isotopic variability in this region (Li et al. 2017; Zhang et al. 2010). These studies have only depended on the synoptic timescale, which has a limited ability to explore the variability of stable isotopes in precipitation. In order to better fill the knowledge gaps, we present four years' daily precipitation isotopic data from the study site to explore atmospheric processes and moisture source that drive isotopic variability in this region. The objectives of this study are to: (1) characterize the variations of daily precipitation stable isotopes; (2) explore the relationship of precipitation stable isotopes with moisture sources and local meteorological parameters; (3) investigate the impact of moisture

rainout processes during the monsoon periods via comparing observational data with model results from IsoGSM2 data.

2 Materials And Methods

2.1 Study area

The study site of Tengchong (TC), adjacent to Myanmar, is located in the southwestern region (SW) of Yunnan Province, China. The total area of the Yunnan province is approximately 3.9 $\times 10^5$ km^2 and is an important component of the Yungui Plateau. The local climate is dominated by Indian monsoon, East Asian monsoon, and westerlies (Fig. 1). Monthly average precipitation amount in TC ranges from 15.4 mm in December to 295.7 mm in July with total amount of 1532.4 mm (Fig. 2). The air temperature presents distinct seasonal variations with mean annual temperature of 15.4 °C (Fig. 2). The study site is characterized with evident dry (October to April) and wet (May to September) seasons. According to the historical meteorological data, the mean precipitation amount in the wet season accounts for 84% of the mean annual precipitation.

2.2 Field sampling and analysis

Daily precipitation samples were sampled at the TC meteorological station in Yunnan province during the observation period from 2009 to 2012. A total of 343 precipitation samples was measured for oxygen-18 and deuterium at the TC sampling site, respectively. All precipitation samples were sealed with screw caps, and wrapped with parafilm to prevent sample loss and evaporation prior to analysis. In addition, the duration of each precipitation event, air temperature, relative humidity, and precipitation amount were recorded during the observation period.

Precipitation samples were determined by a liquid water isotope analyzer (LGR-DLT100, USA) at the Key Laboratory of the College of Resources and Environmental Sciences, Hunan Normal University. The measured ratios of the stable isotopes in samples were expressed as parts per thousand of their deviation relative to the Vienna Standard Mean Ocean Water (VSMOW). The measurement precisions for $\delta^{18}O$ and $\delta^{2}H$ were ±0.3 ‰ and ±1 ‰, respectively. Deuterium excess (d-excess) is calculated as $d= \delta^{2}H-8*\delta^{18}O$ to investigate non-equilibrium effects on the isotopic composition of precipitation (Dansgaard 1964).

In addition, monthly precipitation isotope composition data collected at the GNIP Kunming station were used in this study. The 15-year GNIP data were recorded from 1986 to 2003 (absent from 1993 to 1995) along with mean monthly temperature and precipitation amount at the Kunming station.

2.3 HYSPLIT backward trajectories analysis

To determine the origin of air masses and transport paths, air mass back trajectory was calculated for each precipitating day using the Hybrid Single Particle Lagrangian Integrated Trajectory (HYSPLIT) model version 4.0 (Stein et al. 2015). Meteorological data at 1°×1° and 3-hourly resolution from the Global Data Assimilation System (GDAS) were used to drive the HYSPLIT model. Backward trajectory was set for a time period of 10 days and started at 1500 m above ground level. The selection of 1500 m height corresponding to the 850 mb pressure level was considered the major condensation and strong horizontal moisture transport in this region (Breitenbach et al. 2010). Air parcel positions and specific humidity were calculated in the HYSPLIT model. Trajectory frequency passing through a certain 1°×1° box was calculated to visualize the spatial pattern of precipitating air mass transport.

For selected typical precipitation events, ten-day backward trajectories representing daily rainfall samples were calculated as trajectory ensembles. Each including twenty-seven ensemble members released at 12:00 LT on the day of precipitating sample collection. HYSPLIT ensembles analysis was helpful for reducing the uncertainty of a single run for trajectory analysis.

2.4 Models and data sources

To assess the effect of air rainout processes from main moisture source of BoB on the precipitation isotopes variability during monsoon period, three boxes including ocean box (Box 3), land box (Box 2) and site box (Box 1) were designed during the monsoon periods (Fig. S1). The region of BoB was the main moisture source fed the southwest China during the monsoon periods (Seen from backward trajectory discussion later). The moisture suffered fractionation by rainout during advection over the moisture source of BoB (Ocean box) and the land Box (Myanmar) and is further changed by recycling before rainout in the TC study site (Site box). Rayleigh distillation model was considered to explore the step-wise changes in the vapor isotopic composition and then the determination of precipitation isotopes in the TC study site. The detailed description of modeling the isotopic composition in precipitation was listed in the supplementary material.

In this model, some meteorological parameters such as wind speed, relative humidity, specific humidity and the total column water vapor in the atmosphere across BoB and the study region. These variables were produced from the ERA-Interim data set from the European Centre for Medium Weather Forecast with 0.75° × 0.75° spatial resolution (http://www.ecmwf.int/en/research/climate-reanalysis/era-interim). The SST data with 1° × 1° spatial resolution was available from National Oceanic and Atmospheric Administration (NOAA) optimum interpolation SST version 2 (V2) (https://www.ncdc.noaa.gov/oisst/data-access).

Due to the lack of the isotopic compositions of water vapor, the data set of Isotope Global Spectral Model version 2 (IsoGSM2) was used to estimate the rainout fraction, which is compared with the calculated stable isotopes in water vapor from Rayleigh model during the transporting processes. The IsoGSM2 is a water isotope-enabled general circulation model, developed by (Yoshimura et al. 2008). IsoGSM2 has a horizontal resolution of 1.8° × 1.8° and 28 vertical levels, and a time resolution of six hours. IsoGSM2 simulations were used for obtaining estimates of vapor isotopic compositions (Wei et al. 2018).

3 Results

3.1 Precipitation isotopic compositions: daily and seasonality

The wide range of precipitation $\delta^{18}O$ and $\delta^{2}H$ values are observed from 2009 to 2012 (Fig. 3 and Table 1). The full dataset is presented in Table S1. Results show that daily $\delta^{18}O$ values vary from -26.8 ‰ to 4.1 ‰ with an amount-weighted average of -10.1 ‰ and $\delta^{2}H$ values range from -200.9 ‰ to 36.9 ‰ with an amount-weighted average of -70.5 ‰ (Fig. 3 and Table 1). By contrast, precipitation $\delta^{18}O$ and $\delta^{2}H$ values display remarkable seasonality during the observation period. Precipitation $\delta^{18}O$ and $\delta^{2}H$ values are higher in the pre-monsoon period ($\delta^{18}O$= -4.9 ‰ and $\delta^{2}H$= -27 ‰) compared with summer monsoon and Fall-winter periods (Table 1).

Compared with precipitation $\delta^{18}O$ and $\delta^{2}H$, precipitation d-excess values are characterized by relatively low degree of variability across seasons (Fig. 3 and Table 1). Precipitation d-excess mean value (10.8 ‰) is similar to the global average d-excess value (10 ‰, Dansgaard, 1964). Three precipitation events have the highest d-excess values (>20

‰) on 16 Sep. 2011, 19 Jan. and 31 Mar. 2012 (Fig. S2), which is associated with moisture sources from Indian Ocean region with high specific humidity and westerlies from the Mediterranean regions with low specific humidity.

The correlations of daily precipitation $\delta^{18}O$ with precipitation amount and air temperature are shown during the entire period (Table 1). Results show that a significant negative correlation of daily precipitation $\delta^{18}O$ with precipitation amount and air temperature is observed, which is consistent to the monthly variations (Fig. S3). By contrast, a significant correlation of air temperature with precipitation $\delta^{18}O$ is found during the Fall-winter period but not for the pre-monsoon and monsoon periods at the TC site.

3.2 Local meteoric water line

The linear regression relationship between $\delta^{18}O$ and $\delta^{2}H$, the meteoric water line (MWL), provides a useful tool to identify seasonal and spatial patterns of isotopic composition among different regions. The local meteoric water line (LMWL) equations are established from daily precipitation $\delta^{18}O$ and $\delta^{2}H$ during the monitoring period at the TC [($\delta^{2}H$=8.12 (±0.04) $\delta^{18}O$+11.2(±0.4)] (Fig. 4). The slope and intercept of LMWL are close to those of GMWL ($\delta^{2}H$=8 $\delta^{18}O$+10 from Dansgaard, 1964) at the TC site. The slope and intercept of TC LWML is distinctly deviated from the monthly GNIP data of Kunming site [($\delta^{2}H$=6.56 (±0.17) $\delta^{18}O$-2.9(±1.5)]. However, the slope and intercept of LMWL differ among various seasons (Fig. S4). The slope values range from 7.79 to 8.09, and the intercept values vary from 8.5 to 12.1 across seasons. The highest slope value (8.09) is found during the Fall-winter period.

4 Discussion

4.1 Relationships of meteorological parameters with isotopic compositions

In light of the time-varying isotope values in the SW regions described above, the potential relationships between precipitation isotopes and local meteorological parameters were explored at the daily (Table 1) and monthly scale (Fig. S3). Precipitation $\delta^{18}O$ exhibited more significant inverse relationships with precipitation amount and air temperature at the monthly and daily scales, which indicated that air temperature and precipitation amount play important roles in determining the isotopic variability at the TC site. Relatively higher precipitation amount pattern was found from May to October (Fig. 2), which indicates that amount effect largely contribute to isotopic variability (Zhang et al. 2010). The amount effect derived from monthly data suggests that the lighter rainfall with smaller raindrops was more inclined to kinetic fractionation resulting in enriched heavy isotope ratios below the cloud in the low-latitude regions (Dansgaard 1964; Risi et al. 2008). The Pearson correlation coefficients of amount effect is remarkably higher at the monthly (r= -0.74, $p < 0.001$, Fig. S3) scale than at the daily (r= -0.42, $p < 0.001$, Table 1) scale. The weak correlation between precipitation $\delta^{18}O$ and daily precipitation amount further indicates that local rainout has relatively little impact on cumulative daily precipitation $\delta^{18}O$ values. Similarly, weak correlations between daily precipitation $\delta^{18}O$ and local precipitation amount are also found at other tropical and subtropical sites (Jiao et al. 2019; Lekshmy et al. 2015; Zhou et al. 2019). Hence, $\delta^{18}O$ and $\delta^{2}H$ time-series have to be interpreted with caution in terms of the ‘amount effect’ in this subtropical region.

The significant anti-temperature effect (negative correlation between precipitation $\delta^{18}O$ and air temperature) was also observed (Table 1 and Fig. S3). The correlation between precipitation $\delta^{18}O$ and air temperature is also found in other regions of Yunnan province such as Kunming and Mengzi site (Li et al., 2017). However, a significant negative

between precipitation $\delta^{18}O$ and air temperature was found during the Fall-winter period but not for the pre-monsoon and monsoon periods (Table 1). The contrasting levels of correlation for the different seasons may indicate that the mechanism of the temperature effect is complex in this region. Some complex local (e.g., vapor recycling or sub-cloud evaporation) and regional atmospheric processes (e.g., convective activity and precipitating rainout) weaken the effect of air temperature on precipitation $\delta^{18}O$ variability, especially the convective systems mask the temperature effect during the monsoon periods (Araguás-Araguás et al. 1998).

The slope value of 8.12 (±0.04) is statistically different to the GMWL at the TC site, indicating little secondary sub-cloud evaporation in the falling rain (Breitenbach et al. 2010; Crawford et al. 2014). However, precipitation $\delta^{18}O$ and $\delta^{2}H$ from the GNIP [($\delta^{2}H$=6.56 (±0.17) $\delta^{18}O$-2.9(±1.5)] are remarkably deviated from the GMWL with a low slope (<8) at the GNIP site of Kunming, suggesting significant evaporative enrichment occurred during rainfall falling process (Fig. 4). The slope of water line was dependent on relative humidity during secondary sub-cloud evaporation, such that evaporation of rainfall droplets after condensation from cloud result in a lower slope value (<8) of LMWL (Dansgaard 1964; Putman et al. 2019; Wu et al. 2015).

4.2 Impacts of moisture sources on precipitation isotopic variability

The time-series of precipitation $\delta^{18}O$ and $\delta^{2}H$ exhibit a clear trend from the enriched isotopic values in the pre-monsoon period to depleted isotopic values in the summer monsoon and Fall-winter period (Fig. 3 and Table 1), which is attributed to changes in moisture source across seasons (Araguás-Araguás et al. 2000; Cai; Tian 2020). One interesting depletion phenomenon is that the most depleted precipitation isotopic values were found in the Fall-winter period ($\delta^{18}O$= -11.9 ‰, $\delta^{2}H$= -83.4 ‰, Table 1), which is consistent to the isotopic results from South Asian regions (Cai; Tian 2020; Yu et al. 2017) showing the lowest isotopic value in the post monsoon periods. This seasonal difference of isotopic compositions is linked to the moisture transport distance (Cai; Tian 2020; Sengupta; Sarkar 2006). The back-trajectory results for all precipitating events across seasons are shown in Figure 5. In the pre-monsoon period, there are two branches of trajectories: one branch from the interior of Arabian Peninsula-Iranian Plateau and another from BoB (Fig. 5a). The higher temperatures and salinities observed in the Red Sea and Arabian Sea with high evaporation rates, where it feeds water vapor to the downstream regions with the enriched isotopic compositions (Ganssen; Kroon 1991). In the summer monsoon period, air trajectories mainly originate from the northern Indian Ocean and crossing the BoB towards the TC site (Fig. 5b). These water vapor experience the rainout distillation processes along the trajectory and then result in the depleted isotopic compositions in precipitation at a given site.

However, in the Fall-winter period, the length of trajectories prolongs, and they split into two branches from the west and east of the study site (Fig. 5c). The east branch of trajectory is from the South China Sea through the Southeast Asia, where the air mass may be supplemented by the depleted isotopic values of water vapor evaporated from surface waters (Han et al. 2018; Yang et al. 2019). For example, Yang et al. (2019) reported that the depleted $\delta^{18}O$ (mean: -13.6 ‰) and $\delta^{2}H$ (mean: -97.4 ‰) values of Lancang river water originated from Qinghai–Tibetan Plateau were observed, which partly contribute to moist vapor with the depleted isotopic values. The other west branch mostly passes through the northern part of India Peninsula, where the Indus and Ganges rivers bring huge quantity of runoff from Himalaya (Kumar et al. 2019; Lambs et al. 2005; Tripti et al. 2019). The complex river systems feed the isotopic compositions of evaporated water vapor into the air mass trajectory. Kumar et al. (2019) have demonstrated that the river water $\delta^{18}O$ values are influenced by meltwater from high elevated regions with low isotopic values. In

addition, spatial distribution of moisture sources for precipitation at TC site shows that the distance between TC and moisture source is longest from the northern region of Africa in the Fall-winter period, causing the depleted $\delta^{18}O$ values. Hence, these results can partly explain the seasonal precipitation $\delta^{18}O$ pattern resulting from transport distance (Breitenbach et al. 2010; Jeelani et al. 2018).

Previous published literatures have reported that large river systems of Ganges and the Yarlungzangbo-Brahmaputra-Padma follows the intense rainfall and snowmelt on the Tibetan Plateau during the summer monsoon (Breitenbach et al. 2010; Kumar et al. 2019). This runoff is featured by the depleted isotopic values because of the high altitude of precipitation over the Himalaya with great rainout fraction during the monsoon, and the influence of the amount effect over land. Meltwater from ice and snow may also increase the depleted isotopic values of this runoff pouring into the BoB. This isotopic dilution can lead to a decrease in $\delta^{18}O$ values (approximately -1 ‰) of BoB surface water. Some GNIP stations (e.g., Barisal) from the SW regions influenced by Indian summer monsoon also show much greater differences between Fall-winter and summer monsoon period. Hence, BoB freshwater plume to some extent affect the isotopic compositions of precipitation in the downstream regions (Breitenbach et al. 2010; Prasanna et al. 2018). In addition, cyclonic activity is active over the BoB in the Fall-winter period, which leads to the relatively low isotopic values in precipitation (Li et al. 2016; Rahul et al. 2016b). Lekshmy et al. (2015) reported that the increased cyclonic activity also can contribute to the depleted $\delta^{18}O$ values in the Fall-winter rainfall.

4.3 Effects of rainout processes during the monsoon periods

As discussed above, moisture originated from BoB regions largely determine the isotopic compositions of most precipitating events based on HYSPLIT backward analysis during the pre-monsoon and summer monsoon periods (Fig. 5). Air masses from ocean to the terminal site experience rainout, advection and local recycling processes, and thus alter the isotopic compositions in water vapor and precipitation. To assess the influence of these processes on isotopic compositions in precipitation, we design three boxes (ocean, land, and site, Fig. S1) to model in terms of processes including four states: evaporation at the source region, transport of moisture and rainout over ocean and land, moisture recycling via transpiration and evaporation from surface waters in the land, and finally the Rayleigh rainout in the terminal TC sampling site (Fig. 6). The detailed description of modelling isotopic compositions of precipitation at TC is listed in the supplementary materials.

The TC precipitation isotopic compositions are estimated by Rayleigh condensation of the emerging water vapor from the ocean and land boxes. A box of 1°×1° around TC is considered to estimate the rainout fraction and precipitation $\delta^{18}O$ values. In the Rayleigh model for the precipitation isotope, water vapor isotopic composition is considered as an important parameter, which is derived from the calculation of classic Rayleigh fractionation formula and IsoGSM2 data. The spatial pattern of water vapor $\delta^{18}O$ values from IsoGSM2 is shown in Figure S5. The modeled predicted precipitation $\delta^{18}O$ values at TC are more enriched than the observed precipitation $\delta^{18}O$ values (Fig. 7), which may be related with moisture recycling during vapor advection over BoB and land (Myanmar). There is overall similarity in the pattern of variations whereas the modeling results by IsoGSM2 ($r=0.53$) are better matched with Rayleigh model ($r=0.38$) (Fig. 7cd). This discrepancy could be resulted from different uncertainties in the model which are not addressed. Our model calculates the isotopic composition in precipitation based on a set of simple Rayleigh fractionation processes occurring over the ocean and land. To that end, many input parameters are derived from satellite measurements of meteorological variables which are not continuous measurements entailing some uncertainties.

According to the model results, a summary picture can be listed as follows (Fig. 6). The daily rainout fraction over the ocean ranges from 0 to 38% whereas over the land varies between 0 to 62 %. The mean evaporated vapor $\delta^{18}O$ values over the ocean is approximately -10 ± 0.07 ‰, which is similar to the previous results by (Sinha; Chakraborty 2020) showing the similar evaporated vapor $\delta^{18}O$ values (-10.3 ‰). The advection vapor $\delta^{18}O$ values over the ocean vary from -15.1 ‰ to -10 ‰ with an average of -11.5 ±1.0 ‰. The effect of rainout and vapor recycling on advection vapor $\delta^{18}O$ over the land (Myanmar) is significant, resulting in the more depleted $\delta^{18}O$ values of advection vapor (-12.9±1.7 ‰). Finally, the modified advection vapor from land produces rainfall at TC with average $\delta^{18}O$ values of -5.1 ±3.5 ‰. However, the amount-weighted average of -10.2 ‰ because the heavier rainfall give rise to more depletion in precipitation $\delta^{18}O$ (e.g., amount effect). In summary, the rainout effect during the moisture advection and the moisture recycling processes over land box (Myanmar) are two important factors in determining the isotopic composition of TC precipitation originated from BoB.

The aforementioned results identify the underlying factors that determine the precipitation isotopic compositions in the SW regions of China, which may be helpful in the interpretation of paleoproxies. Recently, (Yin et al. 2020) reported that the depleted drip water/speleothem $\delta^{18}O$ values in Maomaotou Big Cave can not reflect the rainfall amount. This difference can now be partly explained by the present results that the observed depletions may be linked to the effect of rainout fraction during the transporting processes rather than the local amount effect. Another potential factor is that moisture recycling from land affects the isotopic composition in precipitation (Corcoran et al. 2019; Rahul et al. 2016a). The recycling estimates varies in the space due to the heterogeneity of the land cover type (e.g., vegetation and water body), which largely contribute to the atmospheric moisture via evaporation and transpiration (Jasechko et al. 2013). Thus, long-term monitoring of precipitation in the monsoon regions is needed in the future, which may be helpful to quantify the two recycling components in the complex monsoon system and provide validation of predictions from the existing models within reasonable uncertainty (Dütsch et al. 2019; Hu et al. 2019).

Conclusions

In this study, daily observations of isotopic compositions ($\delta^{18}O$, $\delta^{2}H$, and d-excess) from 2009 to 2012 in TC sampling site were presented. The relationships between variations of precipitation $\delta^{18}O$ with local meteorological variables (e.g., precipitation amount and air temperature) were investigated to assess the response of precipitation $\delta^{18}O$ to climate changes. In addition, the influence of moisture sources and moisture rainout processes on precipitation variability was identified from the HYSPLIT trajectory data and Rayleigh distillation models. Results showed that precipitation $\delta^{18}O$ exhibited remarkably seasonal variability, with higher values in pre-monsoon period and lower values in the Fall-winter period. The significant negative relationships of precipitation amount and air temperature with precipitation $\delta^{18}O$ were found, indicating that the variability of precipitation $\delta^{18}O$ greatly depended on local climatic conditions. Compared with precipitation processes, the contrasting moisture sources and its transporting distance largely contribute to the seasonal variability of precipitation isotopic compositions. In the summer monsoon period, moisture sources primarily originated from BoB source regions while air masses were derived from the northern region of Africa and East Asia with the longest transporting distance in the Fall-winter period characterized with the depleted $\delta^{18}O$ values. In addition, the precipitating air masses from BoB transporting towards TC sampling site experience precipitation rainout processes during summer monsoon. The rainout effect during the moisture advection and the moisture recycling processes over land box (Myanmar) are two important factors in determining the isotopic composition of TC precipitation. The findings of this study enhance our

understanding of the temporal variations of precipitation stable isotopes at the TC site, and shed a new light on the study of climatic and environmental controls on precipitation stable isotope composition in SW monsoon regions.

Declarations

Acknowledgments

This study was supported by the Strategic Priority Research Program of the Chinese

Academy of Sciences (XDA23020102), and by the Open fund from the State Key

Laboratory of Earth Surface Processes and Resource Ecology (2020-KF-09), by the

National Natural Science Foundation of China (No. 42071145, 41971029 and 41861022), by the Pioneer Hundred Talent Program, Chinese Academy of Sciences

(Y7BR021001).

References

1. Aggarwal PK, Fröhlich K, Kulkarni KM, Gourcy LL (2004) Stable isotope evidence for moisture sources in the asian summer monsoon under present and past climate regimes. *Geophys. Res. Lett.*, 31
2. Aggarwal PK, Coauthors (2016) Proportions of convective and stratiform precipitation revealed in water isotope ratios. *Nature Geosci*, **DOI:10.1038/ngeo2739**
3. Araguás-Araguás L, Froehlich K, Rozanski K (1998) Stable isotope composition of precipitation over southeast Asia. J Geophys Res 103:721–728
4. Araguás-Araguás L, Froehlich K, Rozanski K (2000) Deuterium and oxygen-18 isotope composition of precipitation and atmospheric moisture. Hydrological processes 14:1341–1355
5. Bedaso Z, Wu S-Y (2020) Daily precipitation isotope variation in Midwestern United States: Implication for hydroclimate and moisture source. Sci Total Environ 713:136631
6. Bowen GJ, Cai Z, Fiorella RP, Putman AL (2019) Isotopes in the Water Cycle: Regional- to Global-Scale Patterns and Applications. Annu Rev Earth Planet Sci 47:453–479
7. Breitenbach SFM, Adkins JF, Meyer H, Marwan N, Kumar KK, Haug GH (2010) Strong influence of water vapor source dynamics on stable isotopes in precipitation observed in Southern Meghalaya, NE India. Earth Planet Sci Lett 292:212–220
8. Cai Z, Tian L (2020) What causes the post-monsoon 18O depletion over Bay of Bengal head and beyond? Geophys Res Lett 47:e2020GL086985
9. Cai Z, Tian L, Bowen GJ (2018) Spatial-seasonal patterns reveal large-scale atmospheric controls on Asian Monsoon precipitation water isotope ratios. Earth Planet Sci Lett 503:158–169
10. Cheng H, Coauthors (2016) The Asian monsoon over the past 640,000 years and ice age terminations. Nature 534:640–646
11. Corcoran MC, Thomas EK, Boutt DF (2019) Event-Based Precipitation Isotopes in the Laurentian Great Lakes Region Reveal Spatiotemporal Patterns in Moisture Recycling. Journal of Geophysical Research: Atmospheres 124:5463–5478

12. Crawford J, Hughes CE, Lykoudis S (2014) Alternative least squares methods for determining the meteoric water line, demonstrated using GNIP data. J Hydrol 519:2331–2340
13. Dütsch M, Blossey PN, Steig EJ, Nusbaumer JM (2019) Nonequilibrium Fractionation During Ice Cloud Formation in iCAM5: Evaluating the Common Parameterization of Supersaturation as a Linear Function of Temperature. J Adv Model Earth Syst 11:3777–3793
14. Dansgaard W (1964) Stable isotopes in precipitation. Tellus 16:436–468
15. Ganssen G, Kroon D (1991) Evidence for Red Sea surface circulation from oxygen isotopes of modern surface waters and planktonic foraminiferal tests. Paleoceanography 6:73–82
16. Gao J, Shen SSP, Yao T, Tafolla N, Risi C, He Y (2015) Reconstruction of precipitation δ18O over the Tibetan Plateau since 1910. Journal of Geophysical Research: Atmospheres 120:4878–4888
17. Han G, Lv P, Tang Y, Song Z (2018) Spatial and temporal variation of H and O isotopic compositions of the Xijiang River system, Southwest China. Isotopes Environ Health Stud 54:137–146
18. Hu J, Emile-Geay J, Tabor C, Nusbaumer J, Partin J (2019) Deciphering Oxygen Isotope Records From Chinese Speleothems With an Isotope-Enabled Climate Model. Paleoceanography Paleoclimatology 34:2098–2112
19. Jasechko S, Sharp ZD, Gibson JJ, Birks SJ, Yi Y, Fawcett PJ (2013) Terrestrial water fluxes dominated by transpiration. Nature 496:347–350
20. Jeelani G, Deshpande RD, Galkowski M, Rozanski K (2018) Isotopic composition of daily precipitation along the southern foothills of the Himalayas: impact of marine and continental sources of atmospheric moisture. Atmos Chem Phys 18:8789–8805
21. Jiao Y, Liu C, Gao X, Xu Q, Ding Y, Liu Z (2019) Impacts of moisture sources on the isotopic inverse altitude effect and amount of precipitation in the Hani Rice Terraces region of the Ailao Mountains. Sci Total Environ 687:470–478
22. Kumar A, Sanyal P, Agrawal S (2019) Spatial distribution of δ18O values of water in the Ganga river basin: Insight into the hydrological processes. J Hydrol 571:225–234
23. Lambs L, Balakrishna K, Brunet F, Probst JL (2005) Oxygen and hydrogen isotopic composition of major Indian rivers: a first global assessment. Hydrological processes 19:3345–3355
24. Lekshmy PR, Midhun M, Ramesh R (2015) Spatial variation of amount effect over peninsular India and Sri Lanka: Role of seasonality. Geophys Res Lett 42:5500–5507
25. Li G, Zhang X, Xu Y, Wang Y, Wu H (2017) Synoptic time-series surveys of precipitation δ18O and its relationship with moisture sources in Yunnan, southwest China. Quat Int 440:40–51
26. Li J, Tao T, Pang Z, Tan M, Kong Y, Duan W, Zhang Y (2015) Identification of Different Moisture Sources through Isotopic Monitoring during a Storm Event. J Hydrometeorol 16:1918–1927
27. Li Z, Li T, Yu W, Li K, Liu Y (2016) What controls the interannual variation of tropical cyclone genesis frequency over Bay of Bengal in the post-monsoon peak season? Atmospheric Science Letters 17:148–154
28. Lin W, Wen C, Wen Z, Gang H (2015) Drought in Southwest China: A Review. Atmospheric Oceanic Science Letters 8:339–344
29. Liu J, Song X, Yuan G, Sun X, Yang L (2014) Stable isotopic compositions of precipitation in China. Tellus B: Chemical Physical Meteorology 66:22567
30. Lone AM, Achyuthan H, Chakraborty S, Metya A, Datye A, Kripalani RH, Fousiya AA (2020) Controls on the isotopic composition of daily precipitation characterized by dual moisture transport pathways at the monsoonal margin region of North-Western India. J Hydrol 588:125106

31. Pausata FSR, Battisti DS, Nisancioglu KH, Bitz CM (2011) Chinese stalagmite δ18O controlled by changes in the Indian monsoon during a simulated Heinrich event. Nat Geosci 4:474–480
32. Prasanna K, Ghosh P, Bhattacharya SK, Rahul P, Yoshimura K, Anilkumar N (2018) Moisture rainout fraction over the Indian Ocean during austral summer based on 18O/16O ratios of surface seawater, rainwater at latitude range of 10°N–60°S. J Earth Syst Sci 127:60
33. Putman AL, Fiorella RP, Bowen GJ, Cai Z (2019) A Global Perspective on Local Meteoric Water Lines: Meta-analytic Insight Into Fundamental Controls and Practical Constraints. Water Resour Res 55:6896–6910
34. Rahul P, Ghosh P, Bhattacharya SK (2016a) Rainouts over the Arabian Sea and Western Ghats during moisture advection and recycling explain the isotopic composition of Bangalore summer rains. Journal of Geophysical Research: Atmospheres 121:6148–6163
35. Rahul P, Ghosh P, Bhattacharya SK, Yoshimura K (2016b) Controlling factors of rainwater and water vapor isotopes at Bangalore, India: Constraints from observations in 2013 Indian monsoon. *Journal of Geophysical Research: Atmospheres*, 121, 13,936 – 913,952
36. Risi C, Bony S, Vimeux F (2008) Influence of convective processes on the isotopic composition (δ18O and δD) of precipitation and water vapor in the tropics: 2. Physical interpretation of the amount effect. *Journal of Geophysical Research: Atmospheres*, 113
37. Sengupta S, Sarkar A (2006) Stable isotope evidence of dual (Arabian Sea and Bay of Bengal) vapour sources in monsoonal precipitation over north India. Earth Planet Sci Lett 250:511–521
38. Sinha N, Chakraborty S (2020) Isotopic interaction and source moisture control on the isotopic composition of rainfall over the Bay of Bengal. Atmos Res 235:104760
39. Stein AF, Draxler RR, Rolph GD, Stunder BJB, Cohen MD, Ngan F (2015) NOAA's HYSPLIT Atmospheric Transport and Dispersion Modeling System. Bull Am Meteor Soc 96:2059–2077
40. Tan L, Coauthors (2018) High resolution monsoon precipitation changes on southeastern Tibetan Plateau over the past 2300 years. Quat Sci Rev 195:122–132
41. Tripti M, Lambs L, Moussa I, Corenblit D (2019) Evidence of elevation effect on stable isotopes of water along highlands of a humid tropical mountain belt (Western Ghats, India) experiencing monsoonal climate. J Hydrol 573:469–485
42. Wang S, Zhang M, Che Y, Zhu X, Liu X (2016) Influence of Below-Cloud Evaporation on Deuterium Excess in Precipitation of Arid Central Asia and Its Meteorological Controls. J Hydrometeorol 17:1973–1984
43. Wei Z, Lee X, Liu Z, Seeboonruang U, Koike M, Yoshimura K (2018) Influences of large-scale convection and moisture source on monthly precipitation isotope ratios observed in Thailand, Southeast Asia. Earth Planet Sci Lett 488:181–192
44. Wolf A, Roberts WHG, Ersek V, Johnson KR, Griffiths ML (2020) Rainwater isotopes in central Vietnam controlled by two oceanic moisture sources and rainout effects. Sci Rep 10:16482
45. Wu H, Zhang X, Xiaoyan L, Li G, Huang Y (2015) Seasonal variations of deuterium and oxygen-18 isotopes and their response to moisture source for precipitation events in the subtropical monsoon region. Hydrol Process 29:90–102
46. Xiao X, Haberle SG, Shen J, Yang X, Han Y, Zhang E, Wang S (2014) Latest Pleistocene and Holocene vegetation and climate history inferred from an alpine lacustrine record, northwestern Yunnan Province, southwestern China. Quat Sci Rev 86:35–48
47. Xu X, Tao S, Wang J, Chen L, Zhou L, Wang X (2002) The relationship between water vapor transport features of Tibetan Plateau-monsoon "large triangle" affecting region and drought-flood abnormality of China. Acta

Meteorologica Sinica 60:257–266

48. Yadava M, Ramesh R, Pant G (2004) Past monsoon rainfall variations in peninsular India recorded in a 331-year-old speleothem. The Holocene 14:517–524
49. Yang K, Han G, Zeng J, Liang B, Qu R, Liu J, Liu M (2019) Spatial variation and controlling factors of h and o isotopes in Lancang river water, Southwest China. Int J Env Res Public Health 16:4932
50. Yao T, Thompson LG, Mosley-Thompson E, Zhihong Y, Xingping Z, Lin P-N (1996) Climatological significance of δ18O in north Tibetan ice cores. Journal of Geophysical Research: Atmospheres 101:29531–29537
51. Yao T, Coauthors (2013) A review of climatic controls on δ18O in precipitation over the Tibetan Plateau: Observations and simulations. Rev Geophys 51:525–548
52. Yin J-J, Coauthors (2020) Individual event, seasonal and interannual variations in δ18O values of drip water in Maomaotou Big Cave, Guilin, South China, and their implications for palaeoclimatic reconstructions. Boreas 49:769–782
53. Yoshimura K, Kanamitsu M, Noone D, Oki T (2008) Historical isotope simulation using Reanalysis atmospheric data. *Journal of Geophysical Research: Atmospheres*, 113
54. Yu W, Coauthors (2017) Precipitation stable isotope records from the northern Hengduan Mountains in China capture signals of the winter India–Burma Trough and the Indian Summer Monsoon. Earth Planet Sci Lett 477:123–133
55. Zhang L, Xiao J, Li J, Wang K, Lei L, Guo H (2012) The 2010 spring drought reduced primary productivity in southwestern China. Environmental Research Letters 7:045706
56. Zhang XP, Liu JM, Wang XY, Nakawo M, Xie ZC, Zhang JM, Zhang XZ (2010) Climatological significance of stable isotopes in precipitation over south-west China. International journal of climatology 30:2229–2239
57. Zhou H, Zhang X, Yao T, Hua M, Wang X, Rao Z, He X (2019) Variation of δ18O in precipitation and its response to upstream atmospheric convection and rainout: A case study of Changsha station, south-central China. Sci Total Environ 659:1199–1208

Tables

Table 1 The summary of the daily precipitation isotopic composition, and the correlation with precipitation amount (P) and air temperature (T) at the TC sampling site.

Periods	$\delta^{18}O$ (‰)	$\delta^{2}H$ (‰)	d-excess (‰)	$\delta^{18}O$ &P	$\delta^{18}O$ &T	$\delta^{18}O$ (‰)		$\delta^{2}H$ (‰)		d-excess (‰)		No.
						Min.	Max.	Min.	Max.	Min.	Max.	
Pre-monsoon	-4.9	-27.0	12.4	-0.56*	-0.17	-14.5	4.1	-114.2	36.9	-8.0	22.3	85
Summer monsoon	-11.3	-80.4	10.0	-0.37*	0.03	-21.6	0.8	-150.3	18.6	-5.4	23.2	204
Fall-winter	-11.9	-83.4	11.6	-0.5*	-0.61*	-26.8	2.5	-200.9	30.6	4.1	24.9	54
All	-10.2	-70.5	10.8	-0.42*	-0.43*	-26.8	4.1	-200.9	36. 9	-8.0	24.9	343

Symbols * and ** represent the significance level of 0.001 and 0.01, respectively. No. represent the number of precipitation samples in different periods.

Figures

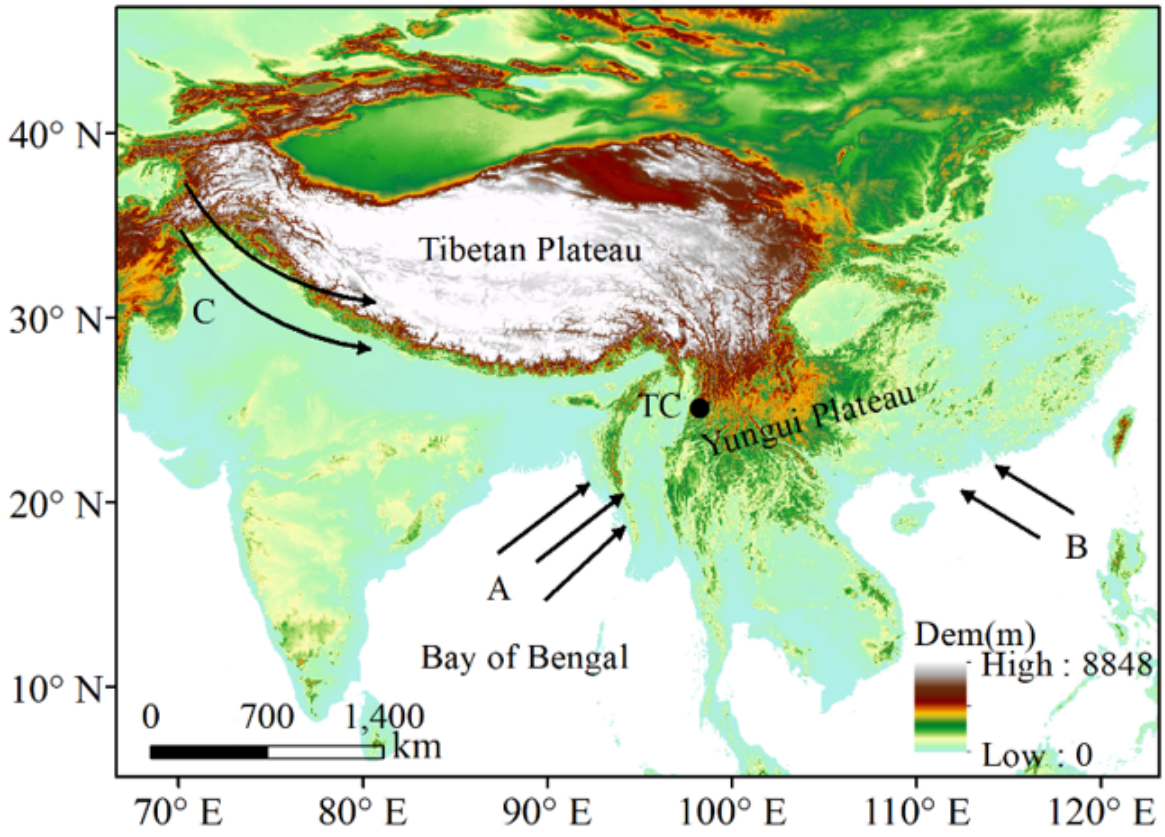

Figure 1

Geographical distribution of study region and precipitation sampling site of Tengchong (TC). The dominant circulation systems (arrows with upper case letter) of the Indian monsoon (A), East Asian monsoon (B), and Westerlies (C). Note: The designations employed and the presentation of the material on this map do not imply the expression of any opinion whatsoever on the part of Research Square concerning the legal status of any country, territory, city or area or of its authorities, or concerning the delimitation of its frontiers or boundaries. This map has been provided by the authors.

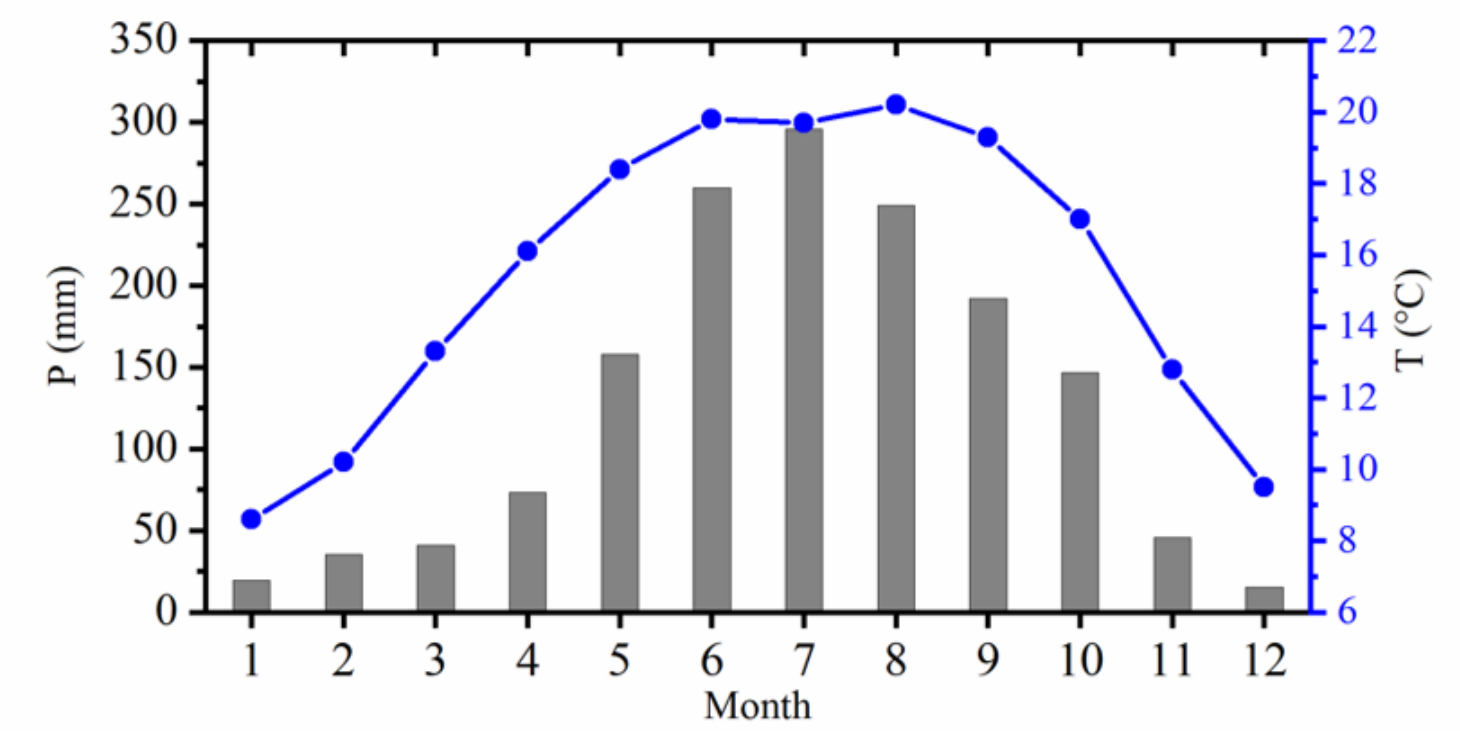

Figure 2

Annual average of monthly precipitation amount (P) and air temperature (T) from 1960 to 2012.

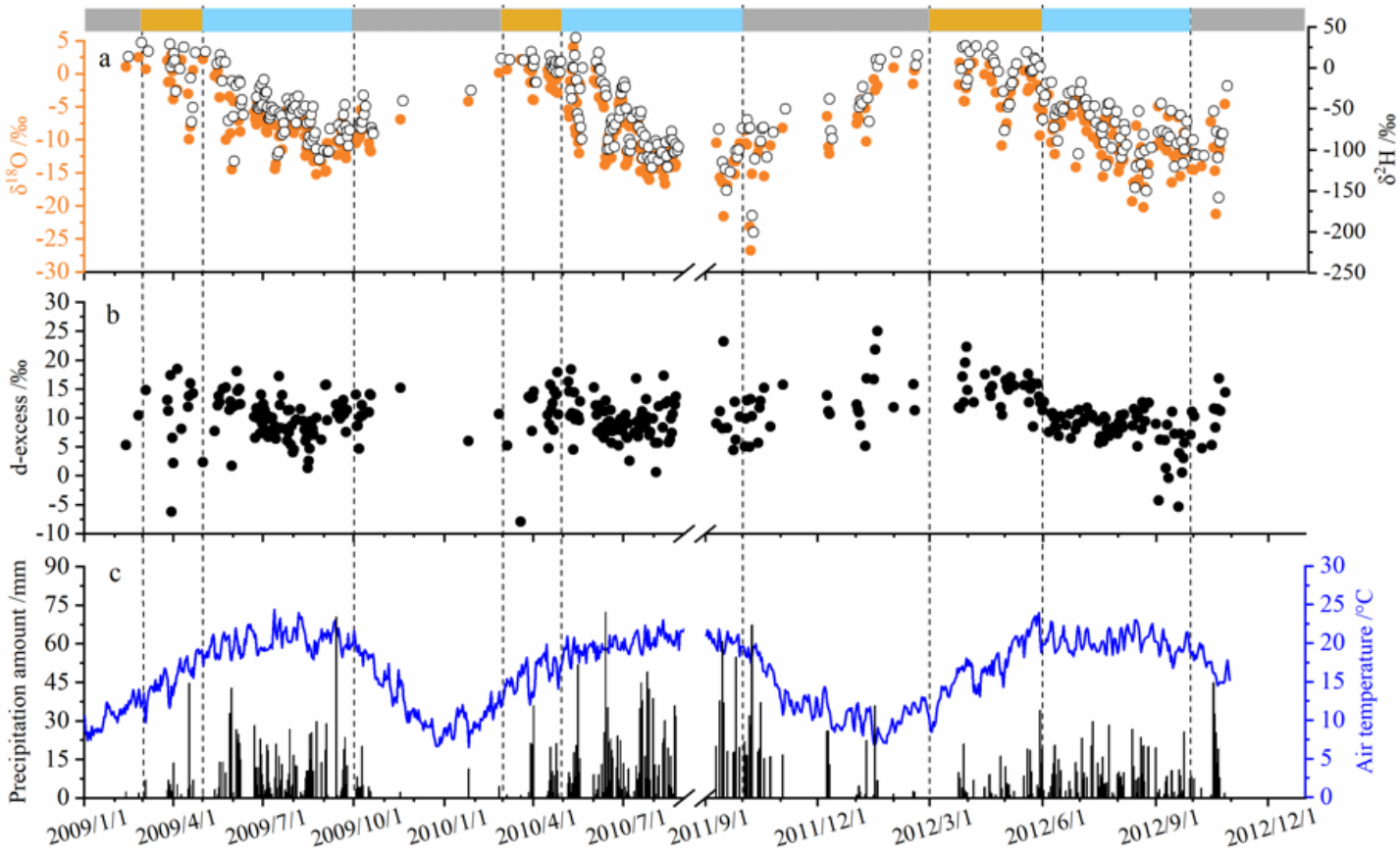

Figure 3

Temporal patterns of daily precipitation δ18O, δ2H, and d-excess values at TC sampling site. Yellow, blue, and gray bars represent the Pre-monsoon, monsoon, and Fall-winter periods, respectively.

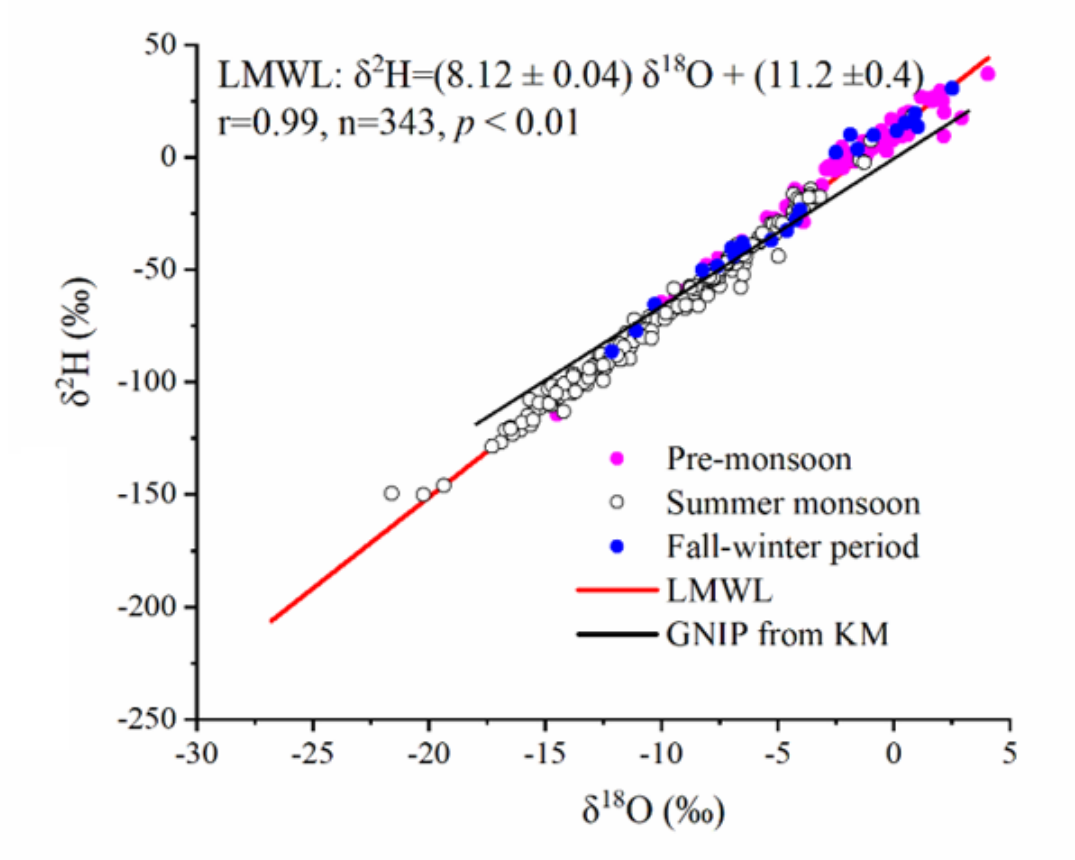

Figure 4

Plots of δ18O and δ2H in precipitation from TC sampling site. KM represents Kunming of the GNIP site.

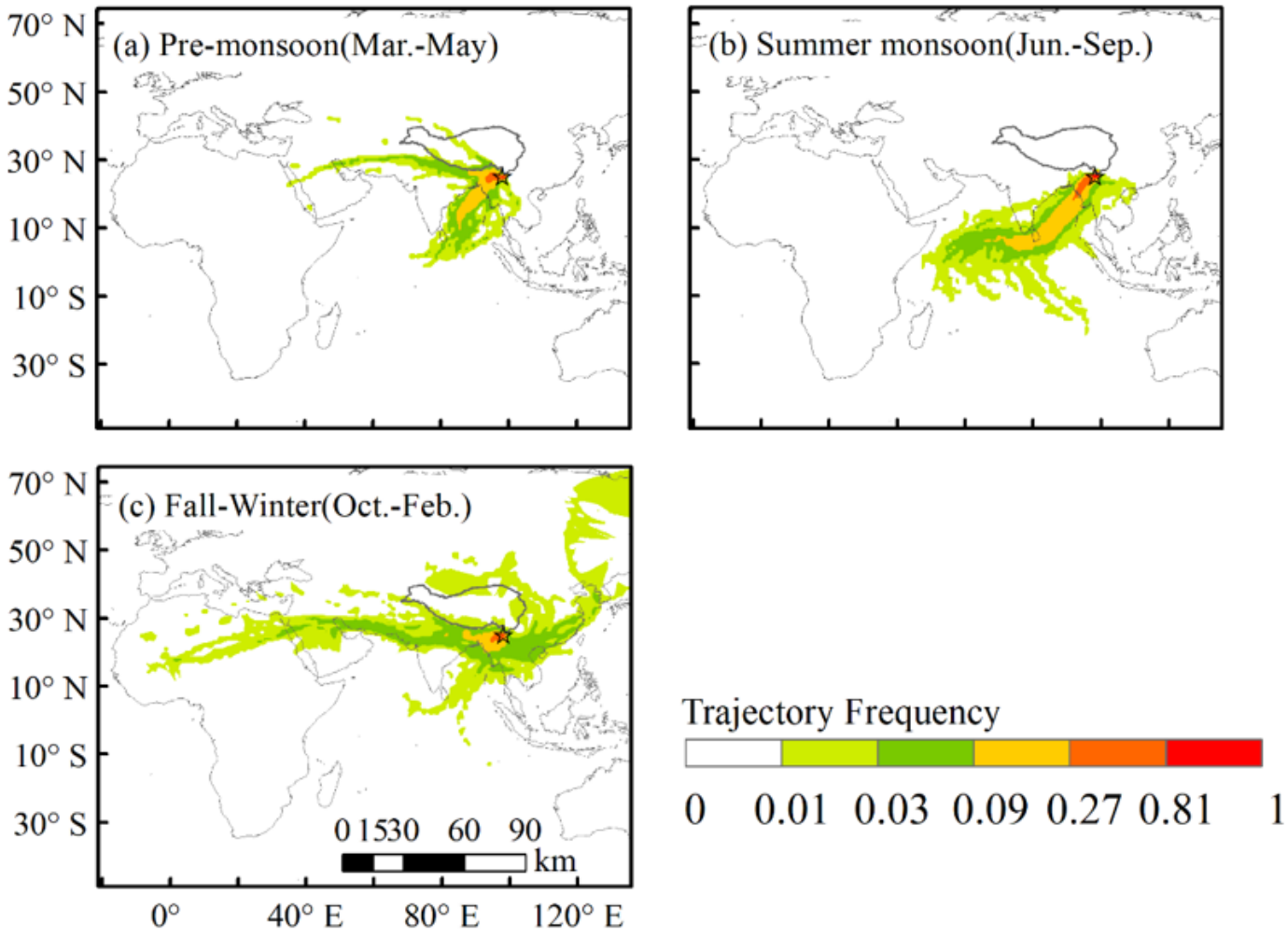

Figure 5

Spatial patterns of 10-day trajectory frequency during pre-monsoon, summer monsoon and Fall-winter periods. Stars indicate the location of TC sampling site. Note: The designations employed and the presentation of the material on this map do not imply the expression of any opinion whatsoever on the part of Research Square concerning the legal status of any country, territory, city or area or of its authorities, or concerning the delimitation of its frontiers or boundaries. This map has been provided by the authors.

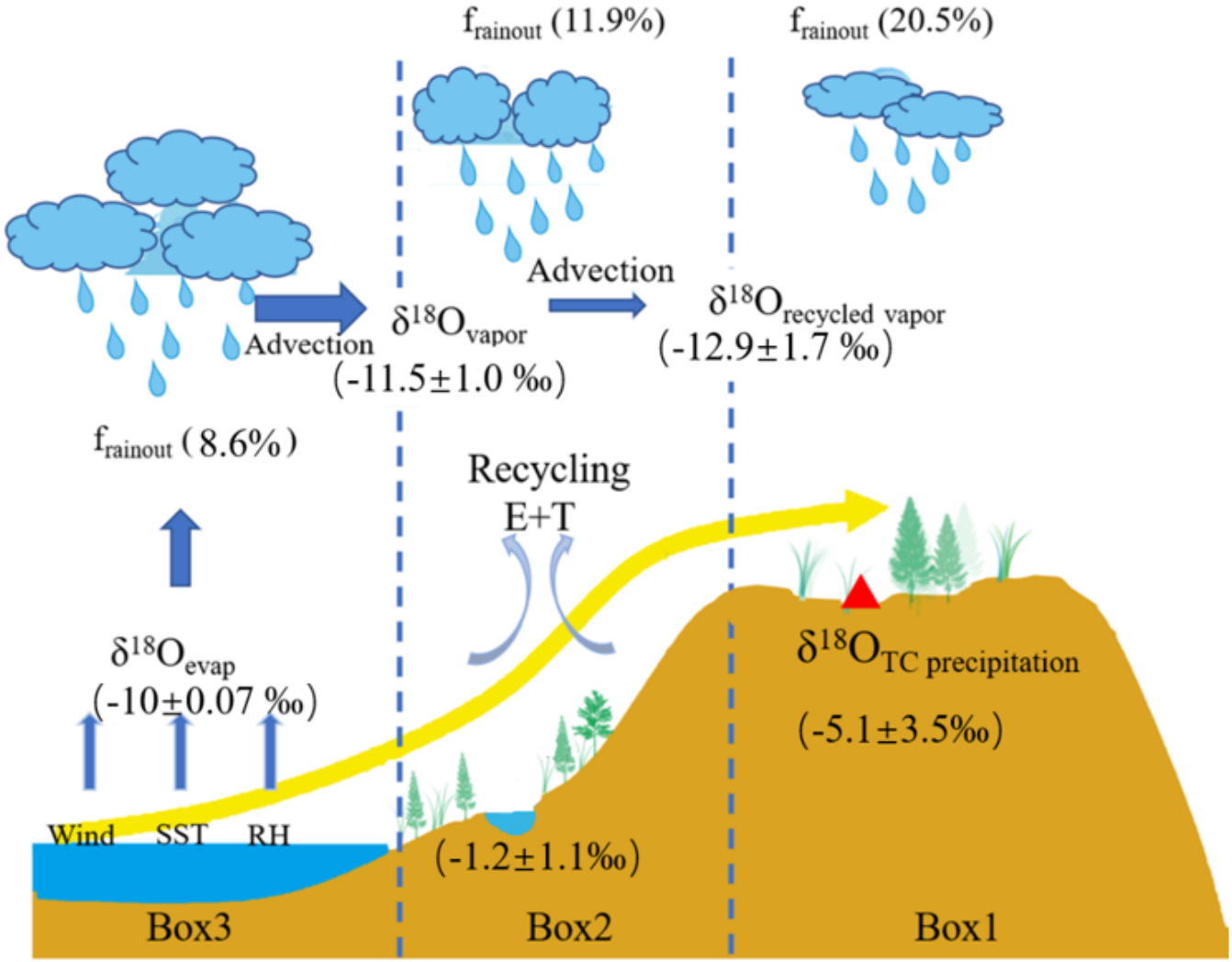

Figure 6

A schematic to illustrate the water vapor stemmed from ocean (Box 3) and its advection towards the land (Box 2). The isotopic compositions of the water vapor are changed by rainout and recycling from transpiration and evaporation from surface waters. This modified water vapor produced precipitation over the TC sampling site (Box 1). The values in brackets represent the mean rainout fraction and δ18O values in water vapor and precipitation, respectively.

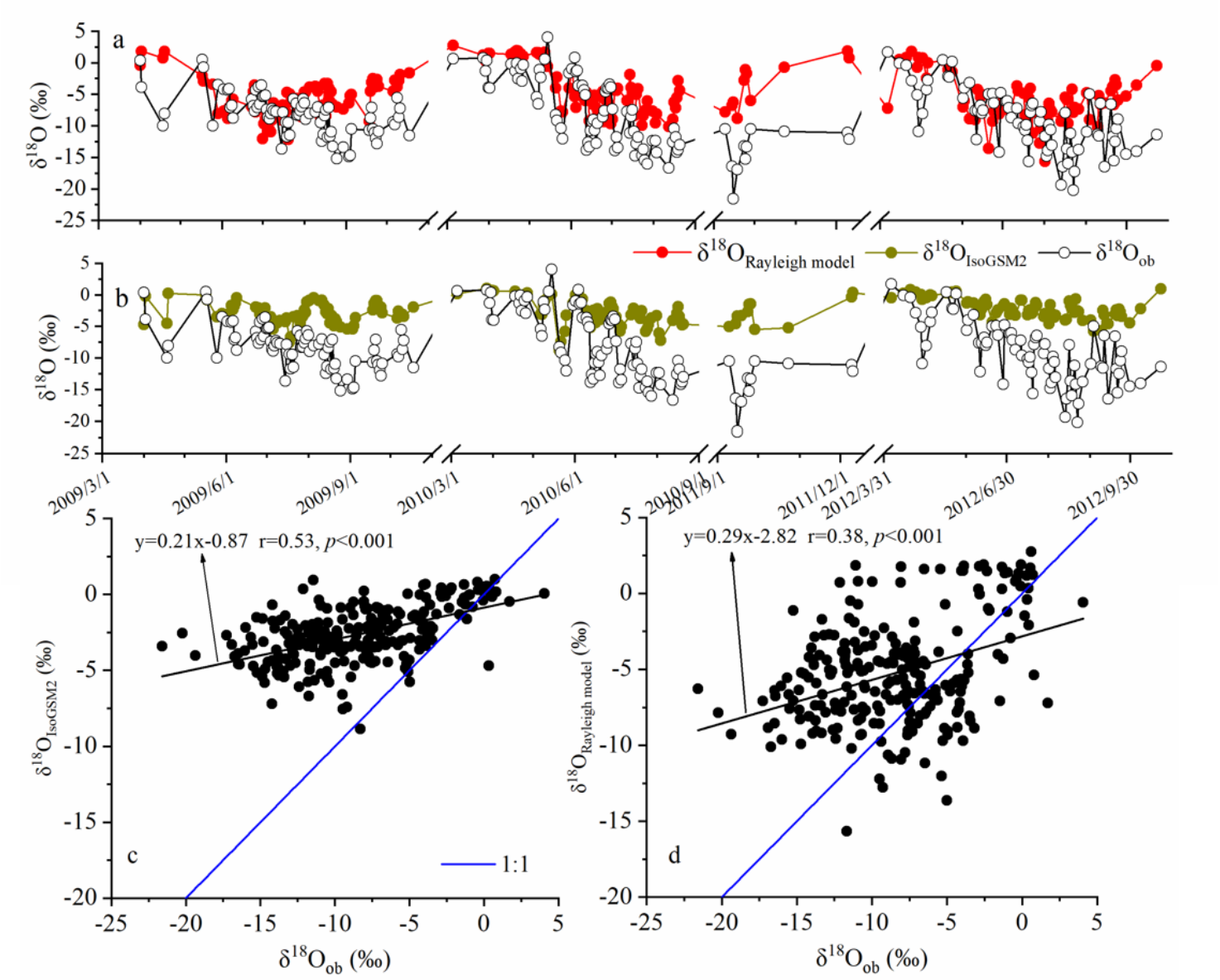

Figure 7

Observed precipitation δ18O values plotted against IsoGSM2 prediction and Rayleigh model at the TC sampling site.

Supplementary Files

This is a list of supplementary files associated with this preprint. Click to download.

- Supplementary.docx